

Contents lists available at ScienceDirect

Applied Surface Science

journal homepage: www.elsevier.com/locate/apsusc



A musical score page showing measures 11 through 14. The vocal line continues with various notes and rests, including a prominent eighth note on 't' in measure 12. The piano accompaniment consists of a bass line and chords, with some notes highlighted in blue.

Zhejiang Provincial Key Laboratory of Plant Evolutionary Ecology and Conservation, Taizhou University, Taizhou 318000, PR China

^aSchool of Engineering, National Engineering and Technology Research Center of Wood-Based Resources Comprehensive Utilization, and Key Laboratory of Wood Science and Technology of Zhejiang Province, Zhejiang Agriculture and Forestry University, Hangzhou, Lin'an 311300, PR China

ARTICLE INFO

Article history:

26 2016 11J 2016
t 18J 2016
b 21J 2016

Keywords:

Keywords:
a s o b t o
o
o o b t
o t s o
o p o t

ABSTRACT

() o o b t o s (-) o t o b o o t ()
o o b y t z t . x o b l o t f i t t
t t - t . o y t y t t t t t o t o -
b o t - t t t t t t t p 2 8 e 3 3 8 , t t
b b t t b y t o o o t o b t t o .
o t p t o t o t y b t t t t o o b o 3 2 - o t
f l o t t o t o b t y. o b o o -
y z b y (o t o s to o y), to o o ()
t y. (y - y) - y o o to o y (x) t o o , -
t y. b t o f i t t y o y o o b o b t -
by o t. - t o o f i f i t y e o t o b o b t o
o - y o t b o b t o t o o b t o .
2016 .. t

1. Introduction

Table 1  (t.%).

3. 81.0 11. 1.5 20. 3.3 17.6 2.7
t o t . [18].

a , t at b o t t t z b o
 o o t y, b b g t y to a
 o b b y t b g e t t ty
 o o t . o i , b z b o t by-
 o x t y p t t t o t o b b y
 f t t . y t b o t , o
 fi t o t o o t o b o b t
 2,12,16,24].

, to t b o (.-) o
t e o t e - - , o
a b y s o f i b r s t t b
o e y s o f i b r s t t b
t . s o , t o x t o b s o b
o u b t t o o o s t b o b t 25-2].
s t t t t t t t o b s t b
(), (), (), () b b
t , b o e o t o b t 14,17,30,31].
o o t t o , y o () b
s t o t o b o t b o t b
f i t y o s t a y o t b t y o t
o 32]. s t y o a t o o t
t t t t o t y o z o o t y
s a t t o b t o - - - 32,33]

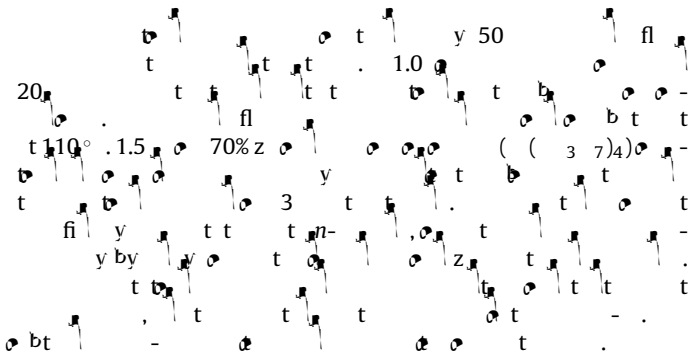
32,53].
a b t o t b o t o - s
a b y o t t t o b z z a o a (x 2)
b o b l t (x) a o o t o t o t . o
t b e o a o b t o t o t o t o z -
o e o b t o t o t o t o o o
o p .
a t o t b ty o 2 o b o -
b t (x) e b t o t o o o o
o b t b t b t o b o
o t , o t o t o t o t o
o b , t t o t o t o t o t b ,
t t t t o o b o o o o o
t t t b t o b o o o o t
g o b y t by x - , o o t -
g o b t y o o t o t y o o t
g o b b a by o t o t b o b t o t (-
a o b t o).

2. Materials and methods

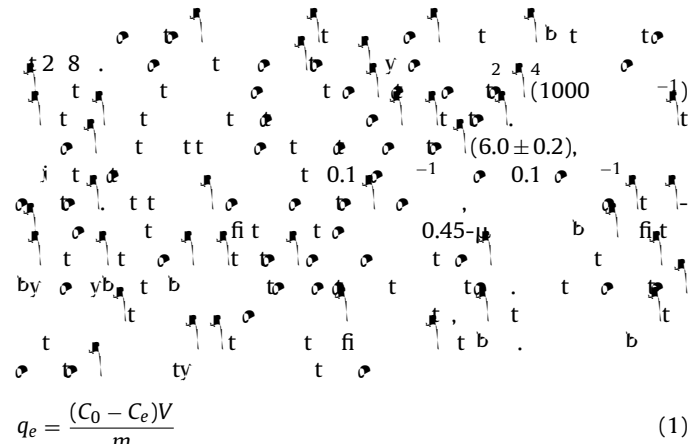
2.1. Materials

A handwritten musical score for piano, page 18, measures 11-12. The score consists of two staves. The top staff starts with a treble clef, a key signature of one sharp, and a common time signature. It contains measures 11 through 12, ending with a repeat sign and a double bar line. The bottom staff starts with a bass clef, a key signature of one sharp, and a common time signature. It continues from measure 12, ending with a final double bar line. The score includes various dynamics like forte, piano, and sforzando, as well as slurs and grace notes.

2.2. Preparation of lignocellulosic butanol residue loading Zr(IV) (LBR-Zr)



2.3. Adsorption studies



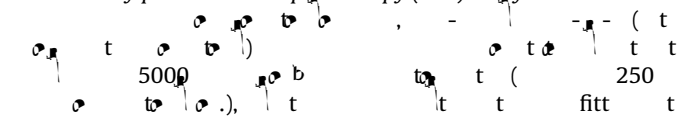
$$q_e = \frac{(\zeta_0 - \zeta_e)V}{m} \quad (1)$$

$$(-1)^{q_e} \left(\begin{array}{ccccccccc} & & & & b_1 & & b_2 & & b_3 \\ (-1) & t & t & t & t & t & t & t & t \\ b & o & o & o & o & o & o & o & o \end{array} \right) V \left(\begin{array}{c} \\ \\ \\ \end{array} \right) \left(\begin{array}{ccccccccc} & & & & b_1 & & b_2 & & b_3 \\ C_e & (-1) & t & t & t & t & t & t & t \\ & & & & o & o & o & o & o \end{array} \right) m \left(\begin{array}{c} \\ \\ \\ \end{array} \right),$$

t o b it o b t t o - o t
 t 2 8 , t o t b 5, 10 20 -1
 t 6.0±0.2 t y. t fit t b t
 1.0-2.0 o t t o t o t o
 t y o o t o t b t y o t
 (2-8) y o o t p t o t t
 40 -1 t o t o t b t 2 8 . t
 t t by 20 -1 t o t o
 t b t t t (2 8, 318 328). t
 o (-, 3-, 4²-, 3²- 3-) t
 o t b 300 -1 t y o t t t
 2 8 t o t o t b o 40 -1 o t
 o b , t o b o 6.0±0.2.

2.4. Adsorbent characterization

2.4.1. X-ray photoelectron spectroscopy (XPS) analysis



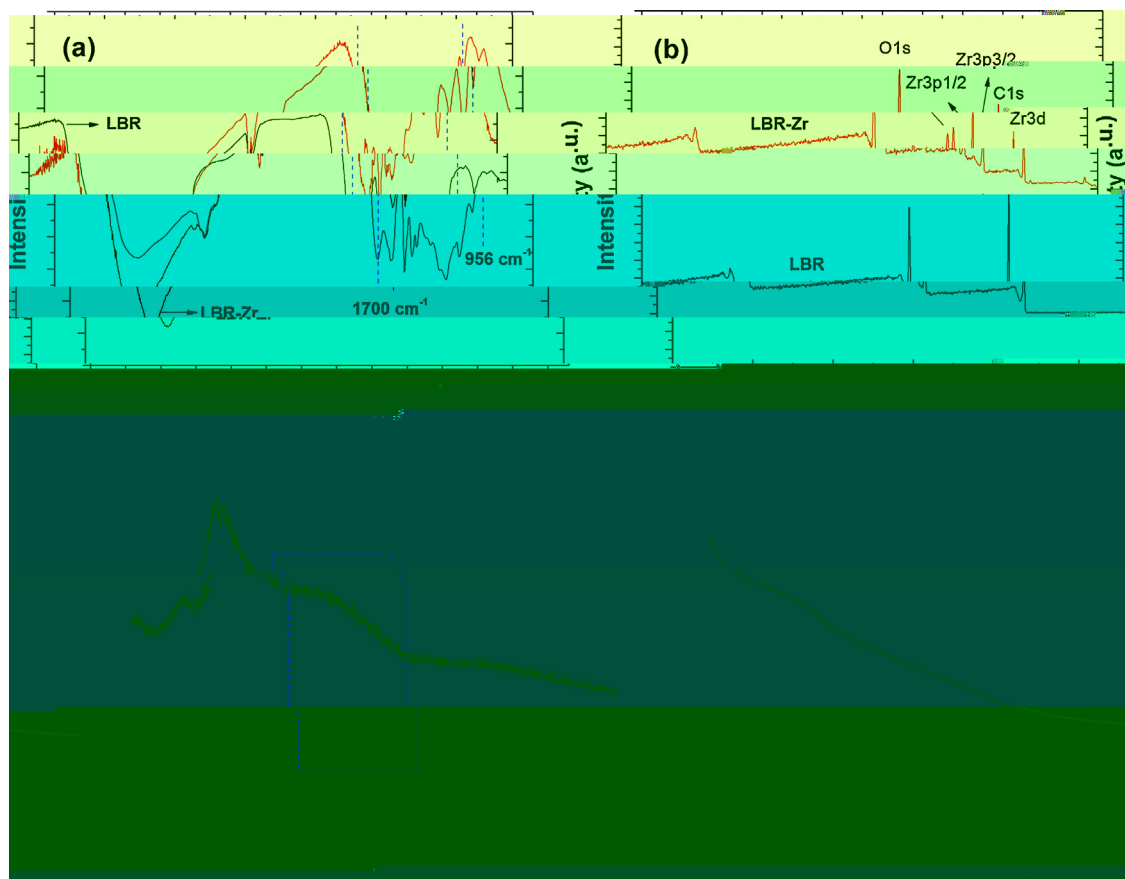
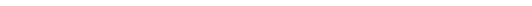


Fig. 1. (a), (b), (c) t_0 , t_1 , t_2 .

Table 2

t t o t o t b p b t.	2 o t t (%)	(2 -1)	(3 -1)
b p o	-	16.38	0.042
o	6. 6	76.38	0.167
t b p			

2.4.2. Fourier transform infrared (FTIR) analysis

2. IR: Fourier transform infrared (FTIR) analysis

 The IR spectrum displays several characteristic absorption bands. A prominent peak is observed around 1100 cm⁻¹, which is typically associated with C-H stretching in aliphatic compounds. Other significant peaks are visible in the fingerprint region between 4000 and 1000 cm⁻¹, though they are less intense than the 1100 cm⁻¹ peak.

2.4.3. X-ray diffractometer (XRD) analysis

$$t \quad 2\theta \quad / \quad - \quad 10-60^\circ \quad t \quad 5^\circ \quad - \quad t \quad \alpha \quad \beta$$

2.4.4. Scanning electron microscopy (SEM) examination with energy-dispersive-X-ray spectroscopy (EDX) analysis

t o b) o o y , - t - (t
t -4800 f t o o ()
t y - y t o o y () t -

2.4.5. Thermogravimetric analysis (TGA)

o t

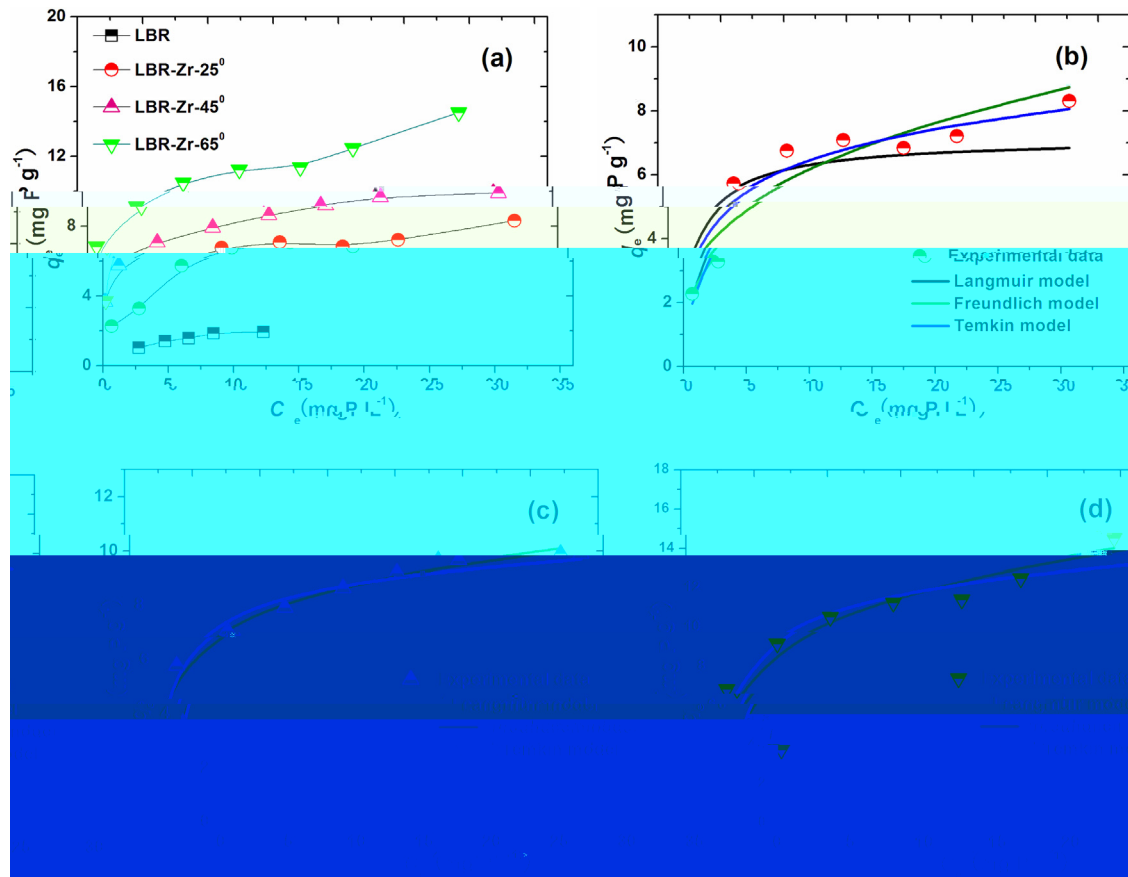


Fig. 2. q_e vs C_e for LBR and LBR-Zr composites at different temperatures. $t = 48 \text{ h}$, $\sigma = 0.625 \text{ g/g}$, $b = 6.0 \pm 0.2 \text{ mg mL}^{-1}$.

	$t = 25^\circ$	$t = 45^\circ$	$t = 65^\circ$	$t = 25^\circ$	$t = 45^\circ$	$t = 65^\circ$	$t = 25^\circ$	$t = 45^\circ$	$t = 65^\circ$
	$t (\text{h})$	$b (\text{mg mL}^{-1})$	(mg g^{-1})	2	2	2	2	2	2
-	2.8	0.64	7.17	0.85	2.6414	2.1	0.442	2.5673	1.5766
-	318	4.51	8.42	0.054	5.2688	5.32	0.32	5.5705	1.141
-	338	2.13	11.78	0.70	6.2336	4.16	0.510	6.8135	1.821

3.2. Structure characterization analysis of LBR-Zr

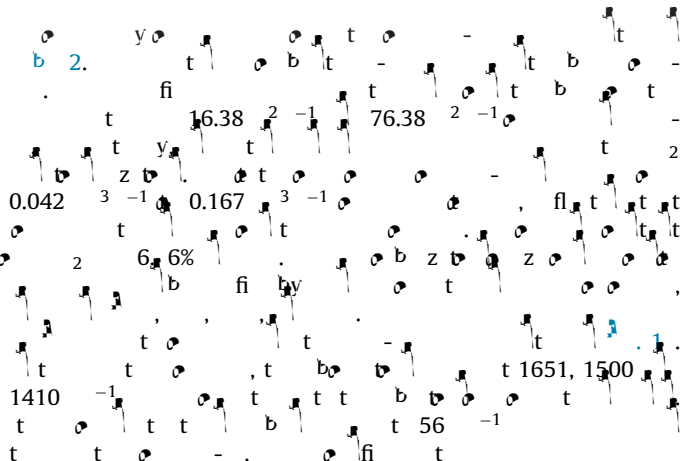


Table 4

b o fi b o s b lt.
b o fi b o s b lt.

3.3. Adsorption isotherm

42]. t, t^y, \dots

43], t^q, t^b, \dots

$$q_e = \frac{Q_0 b C_e}{1 + b C_e} \quad (2)$$

44]. *K_F*

t y b o b o t y t o o n t o e o e b
n t g t o o t t t K³ n t e o e b
ty o b t ty, t y.

$$q_e = K_F C_e^{1/n} \quad (3)$$

t *b* *t* *b* *t* *t.* 45].

$$q_e = A + B - C \quad (4)$$

$\sigma = 6.0 \pm 0.2$ (2). fitt b 3. 2

t 318

0. 054, 0. 32, 0. 800, t y (. 2). t o
t f o t s o b s e - o b b t , b
by i o t o b s f i n t , t t s o b
o o t o a y t o t t b
30]. t o y t t - fi l t y

Table 5

ΔH°	(J σ^{-1})	ΔS°	(J $\sigma^{-1} \text{ K}^{-1}$)
28	-659	0.179	
318			
338	-10.372		

t \rightarrow $z \circ$ t (8.75) b^{-1} , $t \circ b$

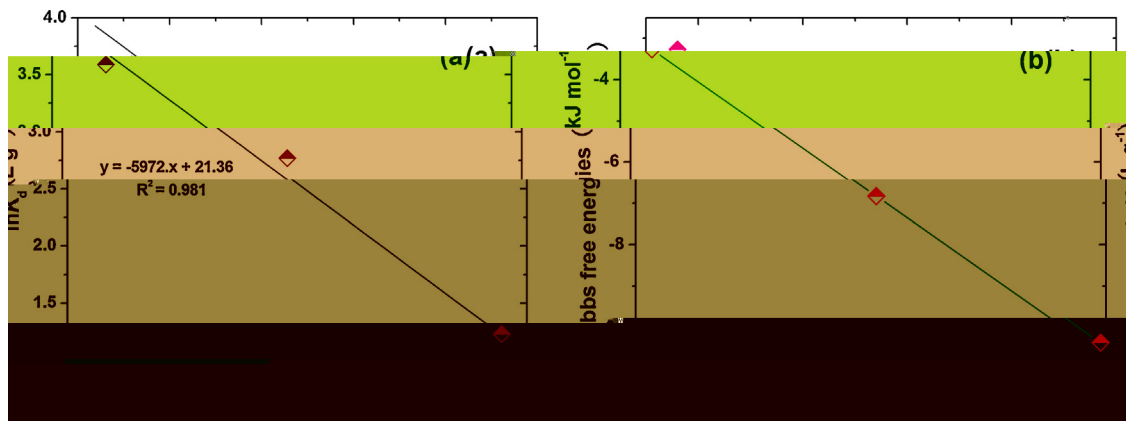


Fig. 3. ΔG° vs $1/T$ (K^{-1}) for the reaction of Fe^{2+} with H_2O_2 in the presence of various organic acids at pH 7. The reaction was monitored by the decrease in absorbance at 420 nm and the increase in absorbance at 424 nm . The reaction mixture contained $10 \text{ mM} \text{Fe}^{2+}$, $10 \text{ mM} \text{H}_2\text{O}_2$, 10 mM organic acid, and $10 \text{ mM} \text{HCl}$ in $50 \text{ mM} \text{Na}_2\text{HPO}_4$ buffer. The reaction was carried out at 25°C for 10 min. The reaction mixture was then diluted 10 times with $50 \text{ mM} \text{Na}_2\text{HPO}_4$ buffer and the absorbance was measured at 420 nm and 424 nm .

	t	σ	t	b	$($	$-1)$	t	σ	t	b	$($	$-1)$	t	σ	t	b	$($	$-1)$			
					q	$($	$-1)$		k_1	$($	$-1)$	2					q	$($	$-1)$		
5					1.	8			0.006		0.837		4.34				0.0283		0.	4.43	
10					3.84				0.00	2	0.	48	6.45				0.0112		0.	6.42	
20					5.05				0.006		0.	41	8.62				0.0075		0.	8.	0

o t o b . t y (ΔH°) bt t t t (5)-(7). K t t b fi t o -
 b t, o t by t b o t b (q)
 b (C) 45,51,52] R t
 (8.314 J o -1 -1) T t t t () t ΔS°
 t to y (J o -1 -1) ΔH° o t t y (J o -1),
 t v.

$$\Delta G^\circ = -RT \ln K \quad (5)$$

$$\Delta G^\circ = \Delta H^\circ - T\Delta S^\circ \quad (6)$$

$$K_d = \frac{\Delta S^\circ}{R} - \frac{\Delta H^\circ}{RT} \quad (7)$$

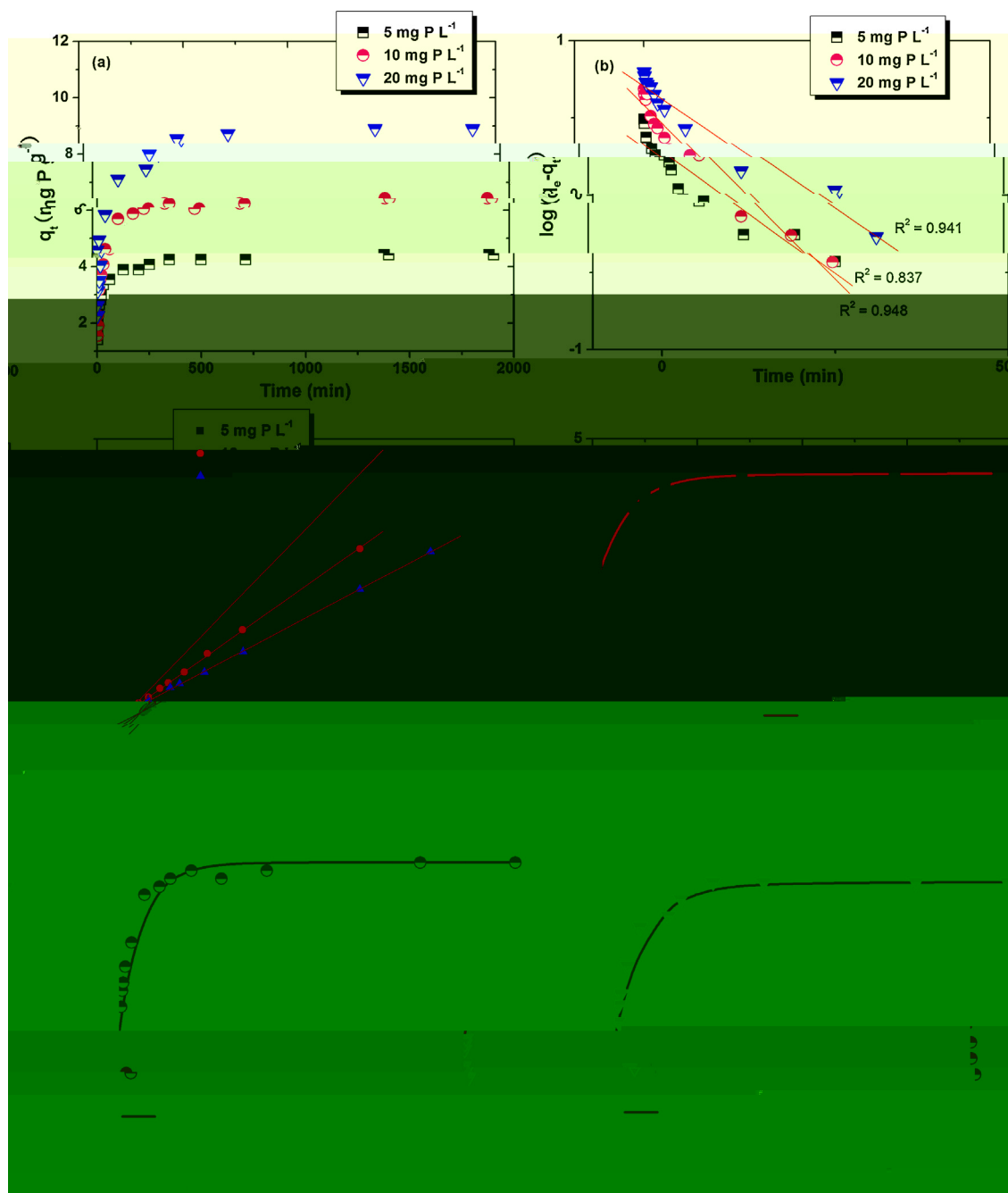


Fig. 4. Adsorption isotherms and kinetics for phosphate adsorption onto a material at different initial phosphate concentrations: (a) 5 mg P L^{-1} , (b) 10 mg P L^{-1} , and (c) 20 mg P L^{-1} .

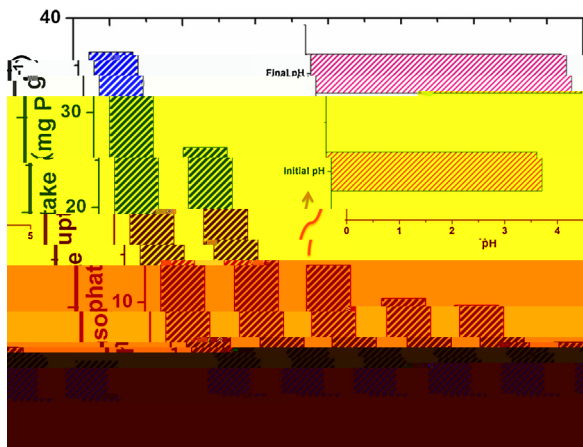


Fig. 5. Phosphate uptake and pH changes over time ($t = 0, 0.5, 1, 2, 4, 120, 24 \text{ h}$).

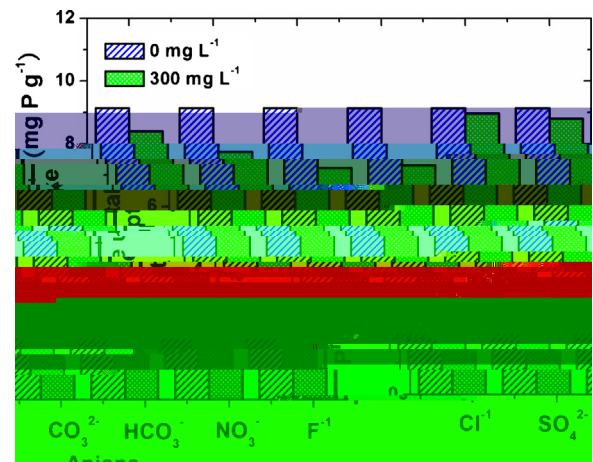
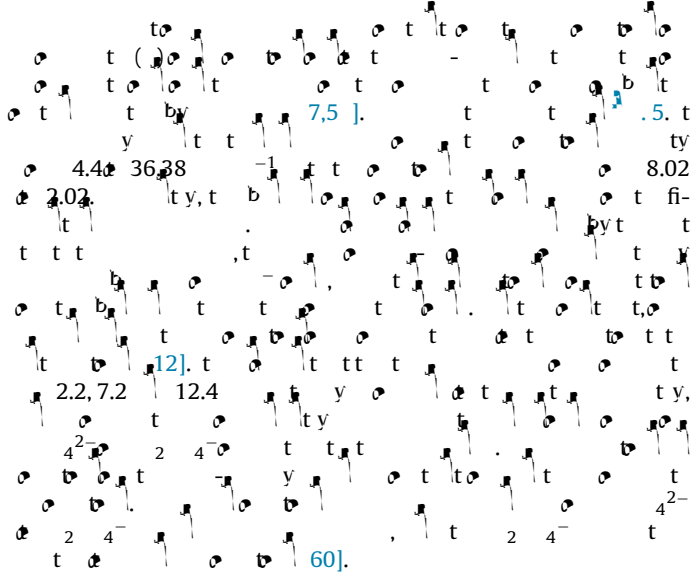
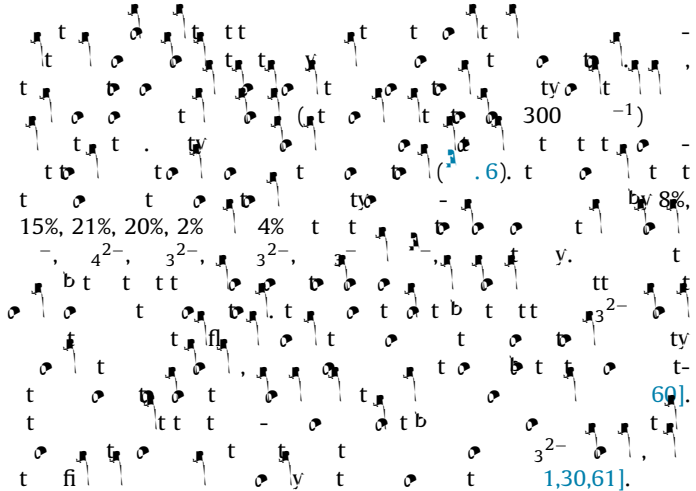


Fig. 6. Phosphate uptake and coexisting anions over time ($t = 0, 0.5, 1, 2, 4, 120, 24 \text{ h}$).

3.6. Effect of pH value



3.7. Effect of coexisting anions



3.8. Analysis of adsorption mechanism of phosphate on LBR-Zr

As shown in Fig. 9, the phosphate adsorption process can be divided into three stages. In the first stage, phosphate ions are adsorbed onto the surface of LBR-Zr by electrostatic interaction [131]. In the second stage, phosphate ions are adsorbed onto the surface of LBR-Zr by coordination interaction [7]. In the third stage, phosphate ions are adsorbed onto the surface of LBR-Zr by hydrogen bonding interaction [12].

3.8.1. SEM-EDX analysis

SEM-EDX analysis was used to study the elemental composition of the LBR-Zr surface. The results showed that the LBR-Zr surface contained elements such as carbon, oxygen, and zinc. The presence of zinc on the surface of LBR-Zr was confirmed by EDX analysis [56].

3.8.2. FTIR spectra analysis

FTIR spectra analysis was used to study the chemical bonds formed between phosphate ions and LBR-Zr. The FTIR spectra showed characteristic absorption bands for phosphate ions, such as the stretching band at 1026 cm⁻¹ and the bending band at 5864 cm⁻¹. The presence of these bands indicated the formation of chemical bonds between phosphate ions and LBR-Zr.

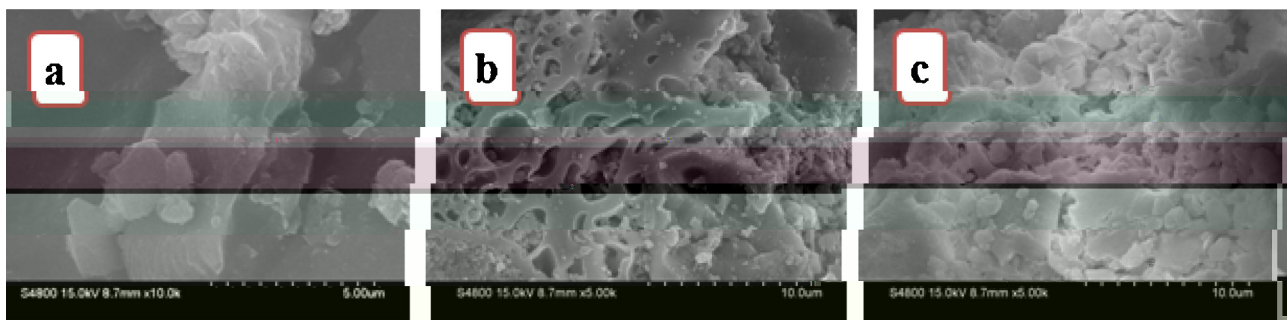


Fig. 7.

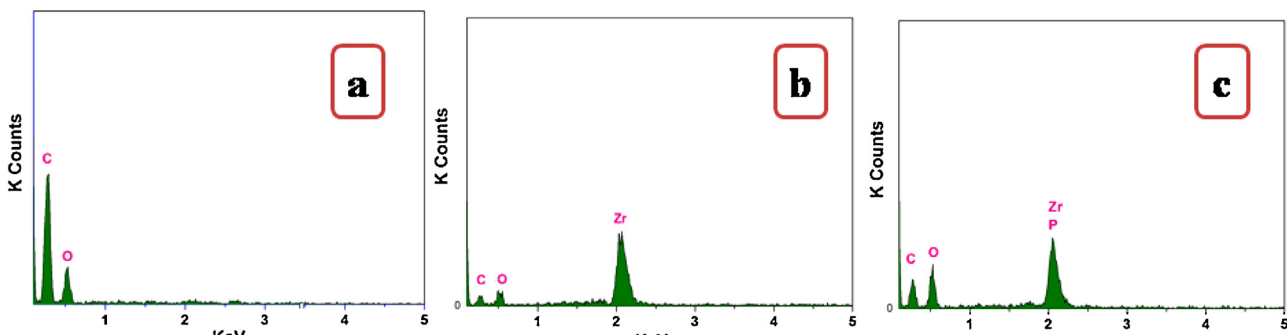


Fig. 8.

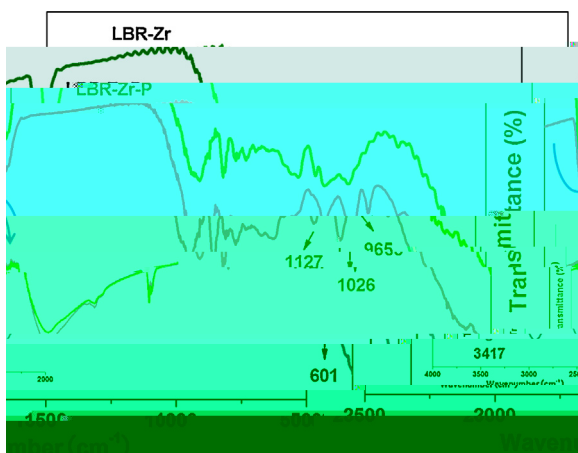


Fig. 9. t e - b e t e t e b

601 -1,
10,24,41]. t tt tt t y o y o o t o
o b t y o t t o t o t o b

3.8.3. XPS spectra analysis

8.8.3. XRD spectra analysis
 o t t t o t o b
 , t - 6¹⁶ t t o t o b
 o yz , t y o t y s t
 o 10, tt b y o e -
 t y 133.6 t o t o o ,
 o o o o t o 45]. o t
 o o t o b p t o t 96m-(6m)TBET/GSt gs
 o t - b o t o b o y 10b
 . t o t t o t o t o 3
 t o b 00021 1.053 160.6037 () i /

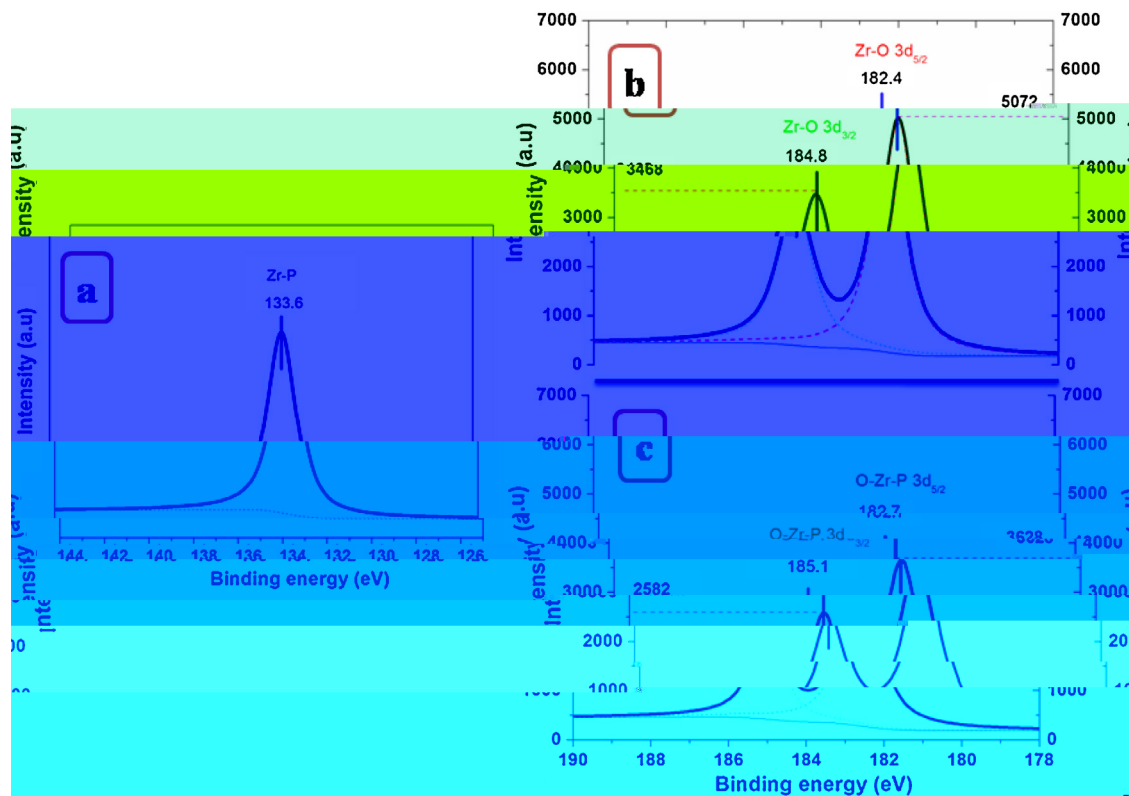


Fig. 10. XPS spectra of (a) Zr-P and (b, c) O-Zr-P.

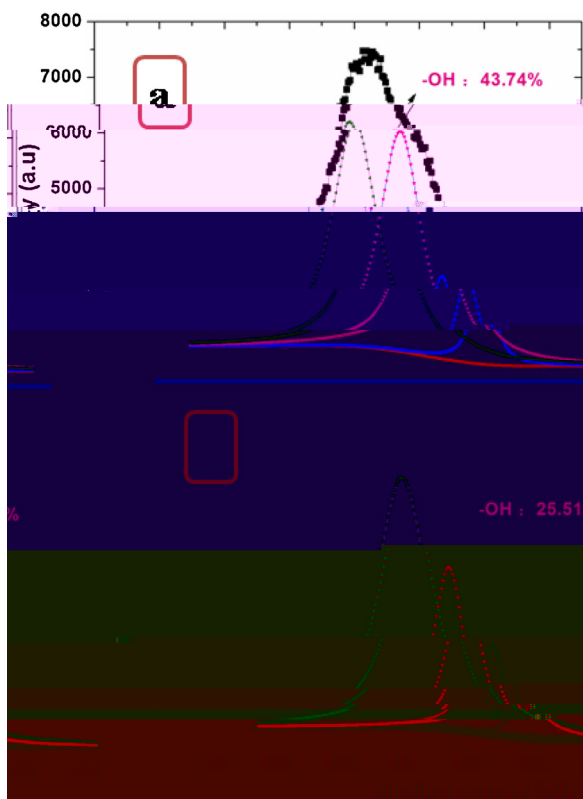


Fig. 11. (b).

24].

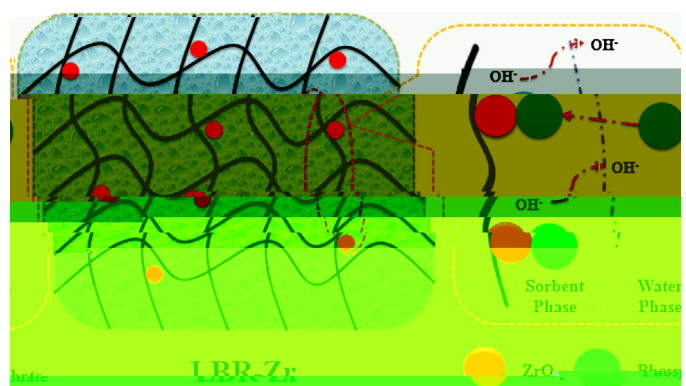
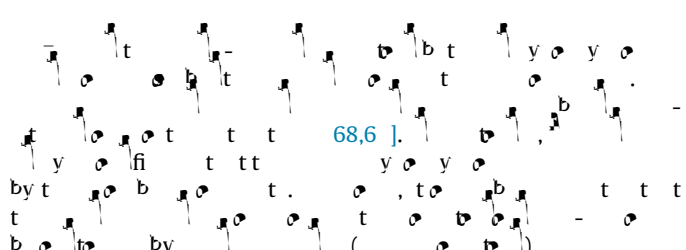


Fig. 12. Schematic diagram of the LRR-ZrO₂ system.



4. Conclusions

This figure is a continuation of the schematic diagram from Fig. 12, showing a larger view of the interface area with various labels for components like 'by', 't', 'y', 'o', 'z', etc.

t y t y t t t o t o b e
t t t o t o t t t 2 8 e 338
t b b b o b b by
t t o - o e b o t o x
by t o b o t o x
t y b t t t o b o t o x
t t t l o t o t o b o t o x
t (- , 4², 3², 3², 3², 3²).
t t y t t t - o t t e
o t t o t t b o t t e
b o y b o b t o o t o t o -
o b o b t o o t t y e o
o b o b t o o t

